



# Synthesis, optimization, DFT/TD-DFT and COX/LOX docking of new Schiff base N'-((9-ethyl-9H-carbazol-1-yl)methylene)naphthalene-2-sulfonylhydrazide

Ahmed Abu-Rayyan<sup>1</sup>, Khalil Shalalin<sup>2</sup>, Mohammed Suleiman<sup>3</sup>, Abed Daraghme<sup>3</sup>, Anas Al Ali<sup>3</sup>, Nawal Aljayyousi<sup>3</sup>, Abdelkader Zarrouk<sup>4</sup>, Mohammad Almaqashah<sup>5</sup>, Ismail Warad<sup>2\*</sup>, Ashraf Sawafta<sup>6\*</sup>

<sup>1</sup>Chemistry Department, Faculty of Arts & Science, Applied Science Private University, Amman P.O. Box 166, Jordan

<sup>2</sup>Department of Dentistry and Dental Surgery, Faculty of Medicine and Health Sciences, An-Najah National University, P.O. Box 7, Nablus, Palestine.

<sup>3</sup>Department of Chemistry, An-Najah National University, P.O. Box 7, Nablus, Palestine.

<sup>4</sup>Laboratory of Materials, Nanotechnology, and Environment, Faculty of Sciences, Mohammed V University in Rabat, Rabat P.O. Box 1014, Morocco.

<sup>5</sup>Department of Biotechnology and Genetic Engineering, Jordan University of Science and Technology, Irbid 22110, Jordan

<sup>6</sup>Biology and Biotechnology Department, An-Najah National University, P.O. Box 7, Nablus, Palestine

\* Corresponding author, Email address: [warad@najah.edu](mailto:warad@najah.edu)

\*\*Corresponding author, Email address: [asawafta@najah.edu](mailto:asawafta@najah.edu)

Received 01 Oct 2023,

Revised 26 Oct 2023,

Accepted 03 Nov 2023

**Citation:** Abu-Rayyan A., Suleiman M., Shalalin K., Daraghme A., Al Ali A., Aljayyousi N., Zarrouk A., Almaqashah M., Warad I., Sawafta A. (2024) Synthesis, optimization, DFT/TD-DFT and COX/LOX docking of new Schiff base N'-((9-ethyl-9H-carbazol-1-yl)methylene)naphthalene-2-sulfonylhydrazide, *Mor. J. Chem.*, 12(1), 78-88

**Abstract** Condensing naphthalene-2-sulfonylhydrazide with 9-ethyl-9H-carbazole-1-carbaldehyde starting materials resulting the formation of novel N'-((9-ethyl-9H-carbazol-1-yl)methylene)naphthalene-2-sulfonylhydrazide Schiff base (S.B.) ligand with high yield and without having any unwanted side products. A wide range of physicochemical measurements, such as CHN-EA, UV-Vis., NMR, FT-IR, and ESI-MS were used to extensively investigate the structural properties of the desired S.B. ligand, the highest level of B3LYB/DFT also served to optimize the 3D structure of the S.B. ligand. Moreover, the experimental optical properties via the UV-Vis absorption measurements were compared to the theoretical DFT/TD-DFT study under identical conditions and using The DCM as solvent. Furthermore, to evaluate the prepared S.B. ligand as a future work drug for treating different types of infections, the LOX and COX anti-inflammatory computation capability was evaluated via the in silico molecular docking using the suitable enzymes.

**Keywords:** Schiff base; NMR; LOX/COX; docking; spectral; DFT/TD-DFT.

## 1. Introduction

Due to their numerous uses in a variety of industries, including chemistry, business, healthcare, and pharmacy, interest in these interesting molecules has significantly increased (Boulechfar *et al.*, 2023; Warad *et al.*, 2020). The azomethine (>C=N-) group, as the substituents can include heterocyclic or aryl/alkyl is a good example of what distinguishes Schiff bases (SBs) from other types of bases (Catalano, 2023). Notably, although the nitrogen atom in the identical link has a highly active free pair of electrons capable of finding stable solid complexes with metal ions, moreover, the sp<sup>2</sup>-carbon center

in the imine unsaturated bond is sensitive to nucleophilic addition reactions. Schiff bases have proven to be versatile in a variety of applications, including catalytic activity, corrosion inhibition properties, photosensitizing abilities, fluorescence chemo-sensor devices designed for the sensing of  $M^{2+}$  metal ions, and photosensitizing behavior (Gupta *et al.*, 2008; Afshari *et al.*, 2023; Upendranath *et al.*, 2022). Schiff bases (SBs), which have a wide spectrum of biological functions, have received a lot of attention in the literature. Key enzymes like butyrylcholinesterase (BChE), acetylcholinesterase (AChE), and carbonic anhydrase have been shown to be inhibited by these compounds (Çakmak *et al.*, 2022; El-Azab *et al.*, 2022; Camadan *et al.*, 2022; Barakat *et al.*, 2013). Aside from that, they have shown positive antimalarial, antitumoral, neuroprotective, antimicrobial, antidepressant, antioxidant, antidiabetic, and anti-inflammatory properties (Tople *et al.*, 2023; Yuldasheva *et al.*, 2022; Hamid *et al.*, 2022).

Additionally, it has been discovered that SBs coatings increase material bioactivity, increasing the scope of their possible medical uses (Mondal *et al.*, 2023). The observed biological effects are thought to be caused by the azomethine nitrogen found in SBs, which acts as a site for interacting with different biomolecules, including proteins and amino acids. The development of compounds with noticeably higher activity is typically caused by the formation of relatively stable complexes between SBs and transition metals, the chemistry, materials science, and pharmacology have all identified uses for this phenomenon for various medicinal applications (Tighadouini *et al.*, 2022; Ashraf *et al.*, 2023; Abu-Yamin *et al.*, 2022; Alezzy *et al.*, 2022). Despite the enormous number of produced SBs ligands, there is still a demand for more of these materials due to the diversity of their prospective applications in scientific domain wide range.

In this article, the composition of a new naphthalene-2-sulfonohydrazide S.B was verified using numerous known physical methods, including DFT/TD-DFT and DFT-optimization studies to determine the existence of the favored isomer. Furthermore, the LOX/COX anti-inflammatory aspects of the desired S.B. were investigated theoretically using the in-silico COX/LOX docking technique.

## 2. Materials and Experimental Methods

### 2.1 synthesis of the S.B.

N'-((9-ethyl-9H-carbazol-1-yl)methylene)naphthalene-2-sulfono-hydrazide was successfully formed when 0.1 mmol of 9-ethyl-9H-carbazole-1-carbaldehyde was treated to condensation with an equal quantity of naphthalene-2-sulfonylhydrazide in methanol under reflux conditions for a duration of 5 hours. The reaction mixture was then let to evaporate until all of the solvent had gone away the yield was an admirable 87%. The yellow powder was thoroughly washed with *n*-hexane and water to assure the purity of the resultant chemical product.

Yellow solid; m.p.: 288.0- 290.0 °C; FT-IR (KBr): 3304, 3033, 1745, 1631, 1390, 1309, 162, 880, 579  $\text{cm}^{-1}$ . Calcd. m/z for  $\text{C}_{25}\text{H}_{21}\text{N}_3\text{O}_2\text{S}$ , 427.2, found 428.4,  $[\text{M}+\text{H}]^+$ . Calcd. CHN-EA analysis: C, 70.24; H, 4.95 and N, 9.83, found C, 70.13; H, 4.88 and N, 9.75.  $^1\text{H-NMR}$  ( $\text{CDCl}_3\text{-d}^1$ , 400 MHz),  $\delta$  1.58 (3H, t), 4.55 (2H, q), 7.13-7.95 (14H, m), 8.33 (1H, s, aldy.), and 9.75 (1HN=C, s).

### 2.1. Materials, computations and docking details

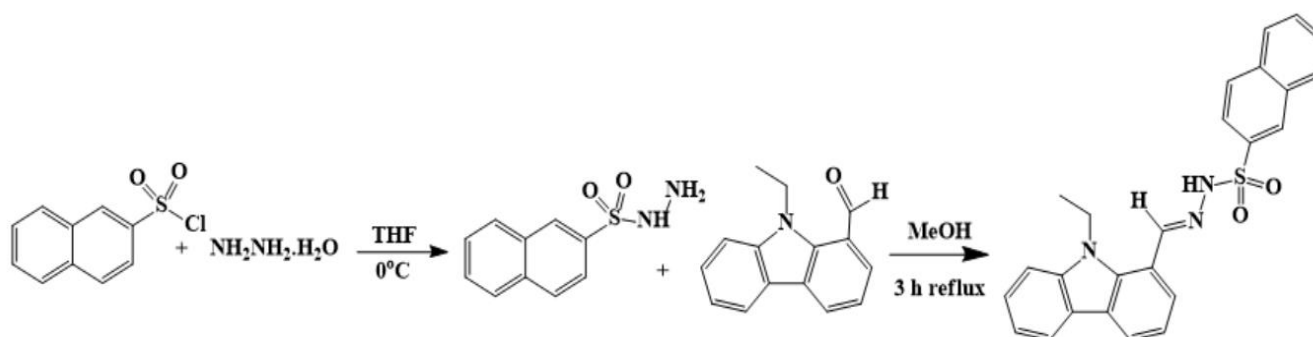
The chemicals were purchased from Sigma-Aldrich and used without further purification. The IR was recorded in solid state in the range of 400-4000  $\text{cm}^{-1}$  using a Shimadzu FTIR-8010 M spectrometer. The  $^1\text{H-NMR}$  were acquired in  $\text{CDCl}_3$  using a Jeol GSX WB spectrometer at 400 MHz. The Gaussian09W program was utilized for the gaseous state DFT calculations at DFT/B3LYP/6-311G (d,p) (Frisch *et al.*, 2009; Al Hamzi *et al.*, 2013; Barhoumi *et al.*, 2020). Using the AutoDock 4.2v

program (Morris *et al.*, 2009; Zaki *et al.*, 2017; El Aissouq *et al.*, 2022), the COX/LOX against the ligand was docked (AlAli *et al.*, 2023a; Rudrapal *et al.*, 2023).

### 3. Results and Discussion

#### 3.1. S.B ligand preparation and identification

The naphthalene-2-sulfonylhydrazide starting material was obtained by combining of naphthalene-2-sulfonyl chloride with an excess amount of  $\text{NH}_2\text{NH}_2\cdot\text{H}_2\text{O}$  at 0 °C in THF (Warad *et al.*, 2020; Daraghmeah *et al.*, 2019). By condensation of 9-ethyl-9H-carbazole-1-carbaldehyde with freshly prepared naphthalene-2-sulfonylhydrazide in an reflux medium using methanol solvent, a novel solid yellow Schiff base N'-((9-ethyl-9H-carbazol-1-yl)methylene)naphthalene-2-sulfonylhydrazide ligand was prepared with high yield 87% (Amereih *et al.*, 2020; Amereih *et al.*, 2021; Warad *et al.*, 2013; Abu-Rayyan *et al.*, 2023; Saleemh *et al.*, 2017) as see (Scheme 1). The product's solubility profile was also examined, and the results showed that it easily to be dissolved in hot water, and other chlorinated solvents like chloroform, although it was hardly soluble in heave ROH, and totally insoluble in hexane.



**Scheme 1:** The desired S.B synthesis.

As described in the experimental section, the synthesized Schiff base was thoroughly characterized via several available analytical tools, such as NMR, UV-Vis., FT-IR spectroscopy, CHN elemental analysis, and ESI-MS.

#### 3.2. DFT-optimization

To optimize the desired S.B., the DFT mode optimization was computationally perfumed via B3LYP/6-311 basis set level. The theoretical calculations confirmed the condensation reaction occurred and the imine  $>\text{C}=\text{N}$ - unit formation as observed in (Scheme 1). Figure 1 shows the S.B. with E-isomer structure as the stable optimized isomer over the Z-isomer one (Amereih *et al.*, 2019, Takfaoui *et al.*, 2014; Lindner *et al.*, 2003). All the dihedral angles, angles, and bond lengths of the named S.B are illustrated in Table 1.

#### 3.3. UV-Vis and TD-DFT investigations

The exp. UV-vis and theoretical TD-DFT simulations were performed using the same solvent ( $\text{CH}_2\text{Cl}_2$ ) to comprehend the electronic and the optical properties of the desired S.B. Since the desired S.B existence with 5 rings (4 aromatic and 1 heterocyclic) in his backbone, the UV-Vis outcome revealed the presence of 3 absorption band at  $\lambda_{\text{max}} = 231, 266$  and 307 nm, that can be resonated to  $\pi$  to  $\pi^*$  e-transfer (Figure 2).

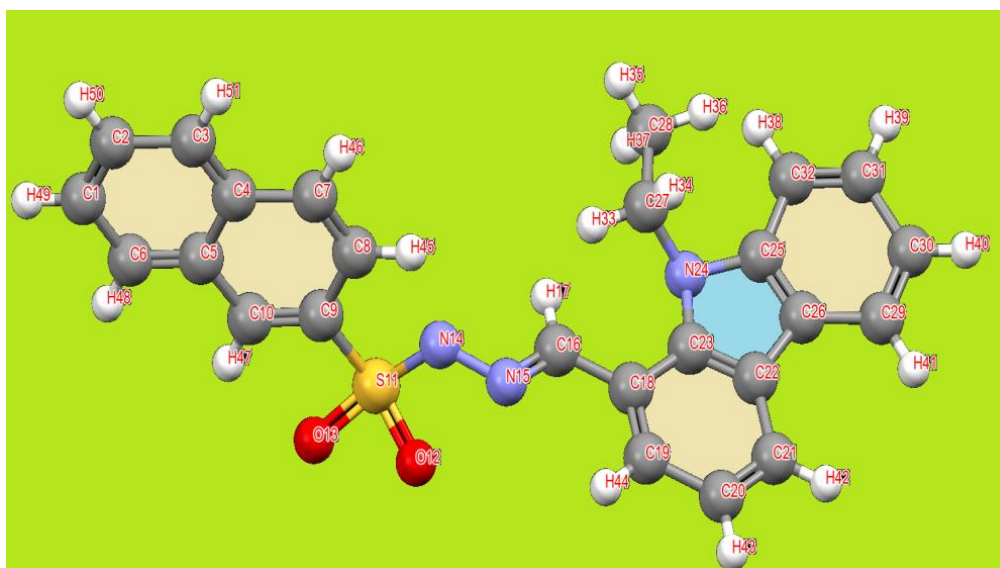


**Figure 1.** DFT/B3LYB E-isomer optimization of the desired S.B.

**Table 1.** Angles, bond lengths and dihedral angles of the desired S.B.

No.	Bond	A	No.	Angle	(°)	No.	Torsion	(°)
1	C1 C2	1.3407	1	C2 C1 C6	119.84	1	C6 C1 C2 C3	0.2
2	C6 C1	1.3418	2	C1 C2 C3	119.79	2	C5 C6 C1 C2	-0.06
3	C2 C3	1.3418	3	C2 C3 C4	120.6	3	C1 C2 C3 C4	-0.06
4	C3 C4	1.3458	4	C3 C4 C5	119.66	4	C2 C3 C4 C5	-0.22
5	C5 C4	1.3478	5	C3 C4 C7	121.16	5	C6 C5 C4 C3	0.36
6	C4 C7	1.3448	6	C5 C4 C7	119.18	6	C6 C5 C4 C7	-180
7	C5 C6	1.346	7	C4 C5 C6	119.42	7	C10 C5 C4 C3	-180
8	C10 C5	1.3457	8	C4 C5 C10	119.54	8	C10 C5 C4 C7	0.45
9	C8 C7	1.3419	9	C6 C5 C10	121.04	9	C3 C4 C7 C8	180
10	C8 C9	1.343	10	C1 C6 C5	120.69	10	C5 C4 C7 C8	-0.19
11	C9 C10	1.3446	11	C4 C7 C8	120.78	11	C4 C5 C6 C1	-0.22
12	C9 S11	1.7938	12	C7 C8 C9	120.5	12	C10 C5 C6 C1	180
13	S11 O12	1.4542	13	C8 C9 C10	118.56	13	C9 C10 C5 C6	180
14	S11 O13	1.4526	14	C8 C9 S11	122.24	14	C9 C8 C7 C4	-0.4
15	S11 N14	1.6974	15	C10 C9 S11	119.2	15	C7 C8 C9 S11	-179
16	N14 N15	1.3521	16	C5 C10 C9	121.44	16	C8 C9 C10 C5	-0.43
17	N15 C16	1.2675	17	C9 S11 O12	107.66	17	S11 C9 C10 C5	179
18	C16 C18	1.351	18	C9 S11 O13	108.3	18	C8 C9 S11 O12	-124
19	C19 C18	1.3523	19	C9 S11 N14	113.15	19	C8 C9 S11 O13	112
20	C23 C18	1.3582	20	O12 S11 O13	114.45	20	C8 C9 S11 N14	-6.79
21	C19 C20	1.3417	21	O12 S11 N14	106	21	C10 C9 S11 O12	57
22	C20 C21	1.3365	22	O13 S11 N14	107.41	22	C10 C9 S11 O13	-67.2
23	C21 C22	1.3369	23	S11 N14 N15	113.74	23	C10 C9 S11 N14	174
24	C22 C23	1.3517	24	N15 C16 C18	135.75	24	C9 S11 N14 N15	61.7
25	C22 C26	1.3389	25	H17 C16 C18	118.72	25	O12 S11 N14 N15	179
26	C23 N24	1.2816	26	C16 C18 C19	119.63	26	O13 S11 N14 N15	-57.8
27	N24 C25	1.2741	27	C16 C18 C23	124.6	27	S11 N14 N15 C16	-174
28	N24 C27	1.4818	28	C19 C18 C23	115.77	28	N14 N15 C16 C18	-2.27
29	C25 C26	1.3386	29	C18 C19 C20	124.07	29	N15 C16 C18 C19	-0.62

30	C25	C32	1.3426	30	C19	C20	C21	119.8	30	N15	C16	C18	C23	179
31	C29	C26	1.3395	31	C20	C21	C22	117.11	31	C20	C19	C18	C16	178
32	C27	C28	1.5341	32	C21	C22	C23	123.7	32	C20	C19	C18	C23	-0.79
33	C30	C29	1.343	33	C21	C22	C26	126.82	33	C22	C23	C18	C16	-178
34	C31	C30	1.3437	34	C23	C22	C26	109.48	34	C22	C23	C18	C19	1.6
35	C32	C31	1.3443	35	C18	C23	C22	119.52	35	N24	C23	C18	C16	1.53
				36	C18	C23	N24	137.43	36	N24	C23	C18	C19	-179
				37	C22	C23	N24	103.04	37	C18	C19	C20	C21	-0.42
				38	C23	N24	C25	115.37	38	C19	C20	C21	C22	0.79
				39	C23	N24	C27	126.36	39	C20	C21	C22	C23	0.07
				40	C25	N24	C27	118.27	40	C20	C21	C22	C26	-180
				41	N24	C25	C26	106.04	41	C21	C22	C23	C18	-1.32
				42	N24	C25	C32	134.42	42	C21	C22	C23	N24	179
				43	C26	C25	C32	119.54	43	C26	C22	C23	C18	179
				44	C22	C26	C25	106.06	44	C26	C22	C23	N24	-0.88
				45	C22	C26	C29	131.81	45	C21	C22	C26	C25	-180
				46	C25	C26	C29	122.13	46	C21	C22	C26	C29	0.36
				47	N24	C27	C28	111.97	47	C23	C22	C26	C25	0.38
				48	C26	C29	C30	118.1	48	C23	C22	C26	C29	-179
				49	C29	C30	C31	120.36	49	C18	C23	N24	C25	-178
				50	C30	C31	C32	120.92	50	C18	C23	N24	C27	2.29
				51	C25	C32	C31	118.94	51	C22	C23	N24	C25	1.14
									52	C22	C23	N24	C27	-178
									53	C23	N24	C25	C26	-0.93
									54	C23	N24	C25	C32	179
									55	C27	N24	C25	C26	179
									56	C27	N24	C25	C32	-1.7
									57	C23	N24	C27	C28	-86
									58	C25	N24	C27	C28	94.4
									59	N24	C25	C26	C22	0.28
									60	N24	C25	C26	C29	-180
									61	C32	C25	C26	C22	-179
									62	C32	C25	C26	C29	0.5
									63	N24	C25	C32	C31	-180
									64	C26	C25	C32	C31	-0.38
									65	C30	C29	C26	C22	180
									66	C30	C29	C26	C25	-0.26
									67	C31	C30	C29	C26	-0.1
									68	C32	C31	C30	C29	0.2
									69	C25	C32	C31	C30	0.04

Likewise, TD-DFT computation reflected also three bands at  $\lambda_{\max}$  at 238 nm assigned to H=>L+1(80%) and H-2=>L (20%), with  $\Delta\lambda= 7$  nm regarding the exp. peak, the second  $\lambda_{\max}$  at 260 nm resonated to H=>L(75%) and H-2=>L+1 (25%) with  $\Delta\lambda= -6$  nm, the third  $\lambda_{\max}$  at 314 nm attributed to H-1=>L(65%) and H-1=>L+1 (35%) with  $\Delta\lambda= 7$  nm shift. The degree of agreement between practical UV-Vis and theoretical TD-DFT studies was more than remarkable, as the shift in absorption maxima  $\Delta\lambda$  did not exceed 7 nm at the greatest value as seen in [Figure 2](#)

### 3.4. COX/LOX Molecular docking

The ligand's anti-inflammatory potential was assessed theoretically using in silico docking studies targeting essential inflammation-related proteins such as COX-2 (pdb ID: 4COX), 5-LOX (pdb ID: 6N2W) and COX-1 (pdb ID: 2OYU), which are all recognized as critical targets for anti-inflammatory medicines (Salehi *et al.*, 2019). In order to determine the nature and the power of interactions as well as the overall binding energy, docking studies were conducted (Toubi *et al.*, 2024; AlAli *et al.*, 2023a; AlAli *et al.*, 2023b; Faris *et al.*, 2023; El Masaoudy *et al.*, 2023). The docking studies considerable H-bond interactions constructed between the ligand and the target enzymes as the key to evaluating the power and nature of binding with the nearby amino acids (Figure 3c-f). Notably, the ligand had differential binding sites for various enzymes: for COX-1 and COX-2, it occupied the groove center of the enzyme body (Figure 3a and 3b), while for LOX, it migrated to a more terminal position (Figure 3c).

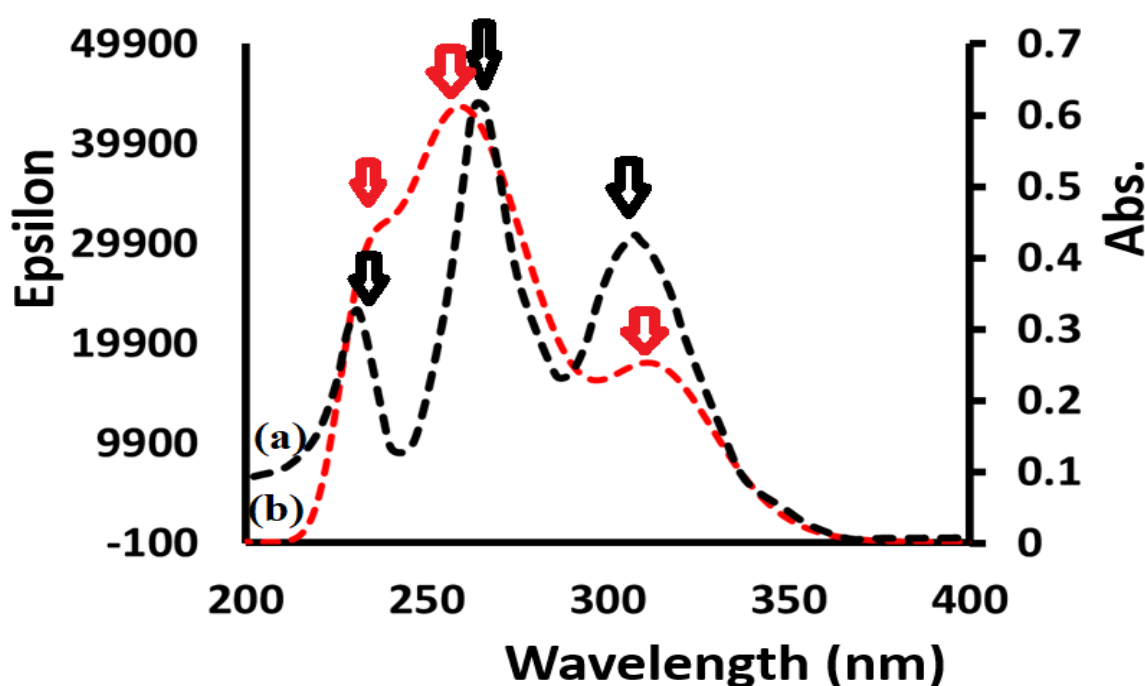


**Figure 2.** (a) UV-Vis, and (b) TD-DFT for the desired S.B in  $\text{CH}_2\text{Cl}_2$  solvent.

In COX-1 (Figure 3d), both O of  $\text{SO}_2$  acted as e-donors to generate H-bond, and when 5-LOX was utilized, one S of  $\text{SO}_2$  was involved in H-bond formation (Figure 3e). In COX-2, the H of NH acted as an e-acceptor to generate a new H-bond interaction (Figure 3f) in addition to the O of  $\text{SO}_2$  interactions. Moreover, the interactions between the S.B molecule and the COX-2 protein had three H-bonds formed, N-H...O of GLN372 with 1.985 Å, O...HZ3 of LYS532 with 2.028 Å, and O...HZ1 of LYS532 with 1.961 Å bond length (Figure 3g). These connections result in the highest binding energy value among enzymes, -12.67 kcal/mol, as shown in (Table 2). COX-1 protein had two H-bonds O...HE2 of HIS388 with 1.897 Å and O...HE2 of HIS207 with 2.059 Å bond distance (Fig.3h) indicating the binding energy of -11.04 kcal/mol. On another hand, the 5-LOX protein had one H-bonds O...HD21 of ASN328 with 2.236 Å (Figure 3i). resulting in the binding energy being the lowest one with -9.94 kcal/mol, as seen in (Table 2). These collected results were consistent with other recently published ones (Elizabeth *et al.*, 2023; Amit *et al.*, 2023).

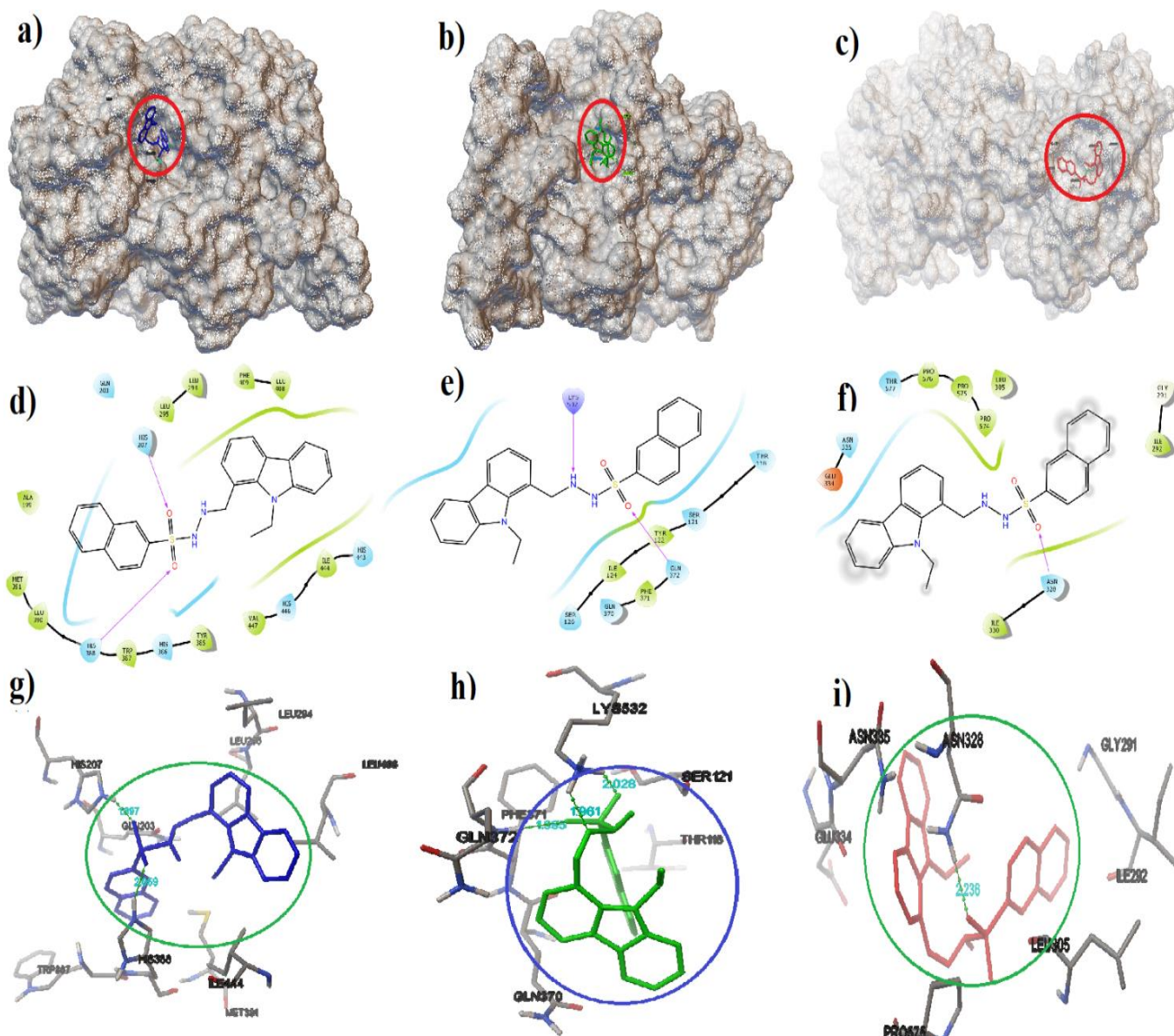


**Figure 3.** Ligand- inflammation enzyme docking result, (a) 2OYU (COX-1), (b) 4COX (COX-2), (c) 6N2W (5-LOX) ligand locations, (d) COX-1, (e) COX-2, (f) 5-LOX 2-D-interactions, (j) COX-1, (h) COX-2, (i) 5-LOX H-bonds natural.

**Table 2.** In silico COX/LOX docking results.

Conf. No.	Protein-Code	B.E (kcal/mole)	L. E	I. C, $\mu\text{M}$ T= 298. 15 K	VdW- Hb- Des-energy kcal/mol	Hb of residues and S.B with bond length ( $\text{\AA}$ )
S.B	COX-1 2OYU	-11.04	-0.36	8.06	-12.53	HIS388:HE2:O (1.897) HIS207:HE2:O (2.059)
	COX-2 4COX	-12.67	-0.41	5.64	-14.16	GLN372:NH:O (1.985) LYS532:HZ1:O (1.961) LYS532:HZ3:O (2.028)
	5-LOX 6N2W	-9.94	-0.32	9.57	-11.42	ASN328:HD21:O (2.236)

## Conclusion

All physico-measurements out consistently confirmed the efficient synthesis of of N'-((9-ethyl-9H-carbazol-1-yl)methylene)naphthalene-2-sulfonylhydrazide ligand, with no side products and a remarkable 87% yield. According to computational DFT-calculation, the E-isomer structure was only slightly favored above the Z-isomer one. Moreover, the UV-Vis spectroscopic analysis revealed that the S.B with three broad-bands which were consistent with the theoretical DFT/TD-DFT computation result.

The ligand's anti-inflammatory activities were theoretically explained using COX/LOX molecular docking experiments. The H-bonding numbers and types reflect the strength of the [ligand: enzyme] complexes interactions. When COX-2 was docked with the S.B ligand, three hydrogen bonds were obtained with a very high bonding energy, whereas only two hydrogen bonds were obtained with a medium energy with the COX-1 enzyme and one hydrogen bond with a lower energy with the LOX-enzyme; thus, the desired ligand can be classified as an excellent COX-2 better than the COX-1 and LOX enzymes. Finally, in silico docking approaches employed in this research paper yielded promising results that could help in understanding the experimental in vitro/in vivo anti-inflammatory medicines behavior.

**Disclosure statement:** *Conflict of Interest:* The authors declare that there are no conflicts of interest.

*Compliance with Ethical Standards:* This article does not contain any studies involving human or animal subjects.

## References

- Abu-Rayyan A., Suleiman M., Daraghmeah A., Al Ali A., Zarrouk A., Kumara K., Warad I., (2023) Synthesis, characterization, E/Z-isomerization, DFT, optical and 1BNA docking of new Schiff base derived from naphthalene-2-sulfonylhydrazide. *Mor. J. Chem.*, 11, 613. <https://doi.org/10.48317/IMIST.PRSM/morjchem-v11i3.39715>
- Abu-Yamin A. A., Abduh M. S., Saghir S. A. M., Al-Gabri N., (2022) Synthesis, characterization and biological activities of new Schiff base compound and its lanthanide complexes. *Pharmaceuticals*, 15, 454. <https://doi.org/10.3390/ph15040454>
- Afshari F., Ghomi E. R., Dinari. M., Ramakrishna S., (2023) Recent advances on the corrosion inhibition behavior of Schiff base compounds on mild steel in acidic media. *ChemistrySelect*, 8, e202203231. <https://doi.org/10.1002/slct.202203231>
- AlAli A., Al-Noaimi M., AlObaid A., Khamees H. A., Zarrouk A., Kumara K., Warad I., Khanum S. A., (2023) Jahn-Teller distortion in SP-like [Cu (bipy)(triamine)]. 2BF<sub>4</sub> complexes with novel NH... F/CH... F synthon: XRD/HSA-interactions, physicochemical, electrochemical, DFT, docking and COX/LOX inhibition. *J. Mol. Liq.*, 387, 122689. <https://doi.org/10.1016/j.molliq.2023.122689>
- AlAli A., Khamees H. A., Madegowda M., Zarrouk A., Kumara K., El-khatatneh N., Warad I., Khanum, S. A. (2023) One-pot reproducible Sono-synthesis of trans-[Br(N∩N')Cu(μBr)<sub>2</sub>Cu(N∩N') Br] dimer:[H... Br S (9)] synthons, spectral, DFT/XRD/HSA, thermal, docking and novel LOX/COX enzyme inhibition. *J. Mol. Struct.*, 1275, 134626. <https://doi.org/10.1016/j.molstruc.2022.134626>
- Alezzy A. A., Alnahari H., Al-horibi S. A., (2022) Short review on metal complexes of Schiff bases containing antibiotic, and bioactivity applications. *J. Chem. Nutr. Biochem.*, 3, 44. <https://doi.org/10.48185/jcnb.v3i2.671>
- Al Hamzi A. H., Zarrok, H. Zarrouk A., Salghi R., Hammouti B., Al-Deyab S.S., Bouachrine M., Amine A., Guenoun F. (2013), The Role of Acridin-9(10H)-one in the Inhibition of Carbon Steel Corrosion: Thermodynamic, Electrochemical and DFT Studies, *Int. J. Electrochem. Sci.*, 8 N<sup>o</sup>2, 2586-2605
- Amereih S., Al Ali A., Zarrouk A., Chetouni A., Kumara K., Lokanath N. K., Warad I., (2019) Synthesis, XRD, DFT-optimization, MEP and Hirshfeld surface analysis of di-μ-Chloro-bis[chloro (1, 10-phenanthroline)Cd(II) dimer. *Mor. J. Chem.*, 7(2), 392-400.



<https://doi.org/10.48317/IMIST.PRSM/morjchem-v7i2.16070>

- Amereih S., Daraghmeah A., Al-Nuri M., Suleiman M., Zarrouk A., Warad I. (2021) Synthesis, NMR, DFT, GRD, MEP, FMO's analysis and comparison of E and Z-isomer of N'-((4-bromothiophen-2-yl)methylene)naphthalene-2-sulfonohydrazide. *Mor. J. Chem.* 9, 232. <https://doi.org/10.48317/IMIST.PRSM/morjchem-v9i2.26239>
- Amereih S., Daraghmeah, A., Warad, I., Al-Nuri, M. (2020). Synthesis, Characterization and Evaluation of Biological Activity of Sulfonylhydrazide Schiff Base (E)- N'-(2,5-dimethoxybenzalidene) naphthalene-2-sulfonohydrazide. *Palest. Tech. Univ. Res. J.* 8, 1.
- Amit A. P., Mubarak H. S., Badrinarayan G. C., Vijay N. B., Baban K. M., (2023) Pyridine-1,3,4-Thiadiazole-Schiff Base Derivatives, as Antioxidant and Antimitotic Agent: Synthesis and in Silico ADME Studies, *Polycycl. Aromat. Compd.*, 43, 1247. <https://doi.org/10.1080/10406638.2022.2026988>
- Ashraf T., Ali B., Qayyum H., Haroone M. S., Shabbir G., (2023) Pharmacological aspects of Schiff base metal complexes: A critical review. *Inorg. Chem. Commun.*, 150, 110449. <https://doi.org/10.1016/j.inoche.2023.110449>
- Barhoumi A., El Idrissi M., Bakkas S., Zeroual A., Tounsi A., El Hajbi A. (2020) A DFT study of the mechanism and regioselectivity of the reaction between diethyl trichloro-methyl phosphonate and diphenyl methyl phosphinite, *Mor. J. Chem.*, 8 No 4, 830-840; <https://doi.org/10.48317/IMIST.PRSM/morjchem-v8i4.20720>
- Barakat A., Al-Noaimi M., Suleiman M., Aldwayyan A.S., Hammouti B., Hadda T.B., Haddad S.F., Boshala A., Warad I. (2013) One Step Synthesis of NiO Nanoparticles via Solid-State Thermal Decomposition at Low-Temperature of Novel Aqua(2,9-dimethyl-1,10-phenanthroline)NiCl<sub>2</sub> Complex. *International Journal of Molecular Sciences*, 14(12), 23941-23954. <https://doi.org/10.3390/ijms141223941>
- Boulechar C., Ferkous H., Delimi A., Djedouani A., Kahlouche A., Boubliia A., Darwish A. S., Lemaoui T., Verma R., Benguerba Y., (2023) Schiff bases and their metal complexes: A review on the history, synthesis, and applications. *Inorg. Chem. Commun.*, 150, 110451. <https://doi.org/10.1016/j.inoche.2023.110451>
- Çakmak R., Başaran E., Sentürk M., (2022) Synthesis, characterization, and biological evaluation of some novel Schiff bases as potential metabolic enzyme inhibitors. *Archiv. Pharm.*, 355, 2100430. <https://doi.org/10.1002/ardp.202100430>
- Camadan Y., Çiçek B., Adem S., Çali Ü., Akkemik E., (2022) Investigation of in vitro and in silico effects of some novel carbazole Schiff bases on human carbonic anhydrase isoforms I and II. *J. Biomol. Struct. Dyn.*, 40, 6965. <https://doi.org/10.1080/07391102.2021.1892527>
- Catalano A., (2023) Schiff bases: A short survey on a promising scaffold in drug discovery. *Curr. Med. Chem.*, 30, 4170. <https://doi.org/10.2174/0929867330666230201121432>
- Daraghmeah, A. F.A. (2019). Synthesis and Characterization of Sulfonylhydrazide-Schiff Bases, their Biological Activities and Molecular Docking. M. Sc Thesis, *An- Najah National University*, 1-87.
- El Aissouq A., Lachhab A., El Rhabori S., Bouachrine M., Ouammou A., & Khalil F., (2022) Computer-aided drug design applied to a series of pyridinyl imidazole derivatives targeting p38 $\alpha$  MAP kinase: 2D-QSAR, docking, MD simulation, and ADMET investigations. *New J. Chem.*, 46, 20786. <https://doi.org/10.1007/s11224-022-01903-5>
- El Masaoudy Y., Tabti K., Koubi Y., Maghat H., Lakhliifi T., & Bouachrine M., (2023) In silico design of new pyrimidine-2, 4-dione derivatives as promising inhibitors for HIV Reverse Transcriptase-associated RNase H using 2D-QSAR modeling and (ADME/Tox) properties. *Mor. J. Chem.*, 11, 300. <https://doi.org/10.48317/IMIST.PRSM/morjchem-v11i2.35455>
- El-Azab A. S., Abdel-Aziz A. A. M., Ghabbour H. A., Bua S., Nocentini A., Alkahtani H. M., Alsaif N. A., Al-Agamy M. H. M., Supuran C. T., (2022) Carbonic anhydrase inhibition activities of Schiff's bases based on quinazoline-linked benzenesulfonamide, *Molecules*, 27, 7703 <https://doi.org/10.3390/molecules27227703>
- Elizabeth N., Pilar M., Michelle M.O., Yesseny V.M., Fernando G., Tamara M., Angel M., Erick F., Carolina M., (2023) Evaluating the inhibitory activity of ferrocenyl Schiff bases derivatives on 5-lipoxygenase: Computational and biological studies, *J. Inorg. Biochem.*, 245, 112233. <https://doi.org/10.1016/j.jinorgbio.2023.112233>
- Faris A., Edder Y., Louchachha I., Ait Lahcen I., Azzaoui K., Hammouti B., Merzouki M., Challioui A., Boualy B., Karim A., Hanbali G., Jodeh S. (2023) From Himachalenes to trans-Himachalol: Unveiling

- Bioactivity through Hemisynthesis and Molecular Docking Analysis, *Scientific reports*, 13, 17653. <https://doi.org/10.1038/s41598-023-44652-z>
- Frisch M. J., Trucks G. W., Schlegel H. B., Scuseria G. E., (2009) Gaussian 09W, Gaussian Inc., Wallingford CT. <http://www.gaussian.com>
- Gupta K. C., Sutar A. K., (2008) Catalytic activities of Schiff base transition metal complexes. *Coord. Chem. Rev.*, 252, 1420. <https://doi.org/10.1016/j.ccr.2007.09.005>
- Hamid S. J., Salih T., (2022) Design, synthesis, and anti-inflammatory activity of some coumarin Schiff base derivatives: In silico and in vitro study. *Drug Des. Develop. Ther.*, 16, 2275. <https://doi.org/10.2147/DDDT.S364746>
- Lindner E., Warad I., Eichele K., & Mayer H. A., (2003) Supported organometallic complexes Part 34: synthesis and structures of an array of diamine (ether–phosphine) ruthenium(II) complexes and their application in the catalytic hydrogenation of trans-4-phenyl-3-butene-2-one. *Inorganica Chim. Acta*, 350, 49. [https://doi.org/10.1016/S0020-1693\(02\)01535-9](https://doi.org/10.1016/S0020-1693(02)01535-9)
- Mondal K., Mistri S., (2023) Schiff base-based metal complexes: A review of their catalytic activity on aldol and Henry reaction. *Comments Inorg. Chem.*, 43, 77. <https://doi.org/10.1080/02603594.2022.2094919>
- Morris G. M., Huey, R., Lindstrom, W., Sanner, M. F., Belew, R. K., Goodsell, D. S. Olson, A. J. (2009) Autodock4 and AutoDockTools4: automated docking with selective receptor flexibility. *J. Comp. Chem.* 16, 2785. <https://doi.org/10.1002/jcc.21256>
- Rudrapal M., Eltayeb W. A., Rakshit G., El-Arabey A. A., Khan J., Aldosari S. M., Alshehri B., Abdalla M. (2023) Dual synergistic inhibition of COX and LOX by potential chemicals from Indian daily spices investigated through detailed computational studies. *Scientific Reports*, 13(1), 8656. doi: [10.1038/s41598-023-35161-0](https://doi.org/10.1038/s41598-023-35161-0)
- Saleemh F. A., Musameh S., Sawafta A., Brandao P., Tavares C. J., Ferdov S., Barakat A., Al Ali A., Al-Noaimi M., Warad I. (2017) Diethylenetriamine/diamines/copper(II) complexes [Cu(dien)(NN)]Br<sub>2</sub>: Synthesis, solvatochromism, thermal, electrochemistry, single crystal, Hirshfeld surface analysis and antibacterial activity. *Arab. J. Chem.* 10 (6) 845. <https://doi.org/10.1016/j.arabjc.2016.10.008>
- Salehi M., Kubicki, M., Galini, M., Jafari, M., Malekshah, R. E. (2019) Synthesis, characterization and crystal structures of two novel sulfa drug Schiff base ligands derived sulfonamide and molecular docking study. *J. Mol. Struct.*, 1180, 595. <https://doi.org/10.1016/j.molstruc.2018.12.002>.
- Takfaoui A., Lakehal I., Bouabdallah I., Halaimia F., Nacer H., Hammouti B., Touzani R. (2014) New imines bearing alkyl armed for catecholase activity, *J. Mater. Environ. Sci.* 5 (3), 753-756
- Tighadouini S., Roby O., Mortada S., Lakbaibi Z., Radi S., Al-Ali A., Warad I., (2022). Crystal structure, physicochemical, DFT, optical, keto-enol tautomerization, docking, and anti-diabetic studies of (Z)-pyrazol β-keto-enol derivative. *J. Mol. Struct.*, 1247, 131308. <https://doi.org/10.1016/j.molstruc.2021.131308>
- Tople M. S., Patel N. B., Patel P. P., Purohit A. C., Ahmad I., Patel H., (2023) An in silico-in vitro antimalarial and antimicrobial investigation of newer 7-chloroquinoline based Schiff-bases. *J. Mol. Struct.*, 1271, 134016. <https://doi.org/10.1016/j.molstruc.2022.134016>
- Toubi Y., Hakmaoui Y., EL Ajlaoui R., Abridgach F., Zahri D., Radi S., Rakib E. M., Lgaz H., Hammouti B. (2024) Unexpected Efficient One-Pot Synthesis, DFT Calculations, and Docking study of new 4-hydroxy-2H-chromen-2-one Derivatives predicted to target SARS-CoV-2 spike protein, *Journal of Molecular Structure*, 2024, 136789, <https://doi.org/10.1016/j.molstruc.2023.136789>
- Upendranath K., Venkatesh T., Nayaka Y. A., Shashank M., Nagaraju G., (2022) Optoelectronic, DFT and current-voltage performance of new Schiff base 6-nitro-benzimidazole derivatives. *Inorg. Chem. Commun.*, 139, 109354. <https://doi.org/10.1016/j.inoche.2022.109354>
- Warad I., Ali O., Al Ali A., Jaradat N. A., Hussein F., Abdallah L., Al-Zaqri N. Alharthi F. A. (2020) Synthesis and spectral Identification of three Schiff bases with a 2-(piperazin-1-yl)-N-(thiophen-2-yl methylene) ethanamine moiety acting as novel pancreatic lipase inhibitors: Thermal, DFT, antioxidant, antibacterial, and molecular docking investigations. *Molecules*, 25, 2253. <https://doi.org/10.3390/molecules25092253>
- Warad I., Daraghmeah A., Al-Nuri M., Zarrouk A., Mousa M., Al-Ali A., Shraim A. M., (2020) Method for synthesizing 1-(naphthalen-2-ylsulfonyl)-3-(thiophen-2-yl) diaziridine. *U.S. Patent* No. 10,836,752 B1.

Washington, DC: U.S. Patent and Trademark Office.

<https://patents.google.com/patent/US10836752B1/en>

Warad I., Eftaiha, A. A. F., Al-Nuri, M. A., Husein, A. I., Assal, M., Abu-Obaid, A., Hammouti, B. (2013) Metal ions as Antitumor Complexes. *J. Mater. Environ. Sci.* 4, 542.

Yuldasheva N., Acikyildiz N., Akyuz M., Yabo-Dambagi L., Aydin T., Cakir A., Kazaz C., (2022) The synthesis of Schiff bases and new secondary amine derivatives of *p*-vanillin and evaluation of their neuroprotective, antidiabetic, antidepressant and antioxidant potentials. *J. Mol. Struct.*, 1270, 133883. <https://doi.org/10.1016/j.molstruc.2022.133883>

Zaki H., Bourass M., Haddaji G., Ouammou K., Benlyass M., & Bouachrine M., (2017) QSAR analyses of Octahydroquinazolinone for insecticidal activity against *spodoptera litura* and its in-silico validation using molecular Docking study. *Mor. J. Chem.*, 5, 202. <https://doi.org/10.48317/IMIST.PRSM/morjchem-v5i1.7834>

---

(2024); <https://revues.imist.ma/index.php/morjchem/index>